

Dual mode operation and control of Fuzzy Logic Controller based Z-source Virtual Synchronous Generator in Solar PV System

D. Jaswanth¹, K. Siva Kumar²

M. Tech Student¹, Professor & HOD²

Department of Electrical and Electronics Engineering, Sri Venkatesa Perumal College of Engineering and Technology, R.V.S.Nagar, K.N.Road, PUTTUR, Chittoor, Andhra Pradesh, India

Article Info

Publication Issue

Volume 10, Issue 1
January-February-2023

Page Number

476-485

Article History

Accepted: 03 Feb 2023
Published: 18 Feb 2023

ABSTRACT

In this research work, proposes a dual mode operation and control of fuzzy logic controller based Z-source virtual synchronous generator in grid connected solar PV system. In grid connected PV systems, maintaining voltage stability is difficult due to sag or swell conditions, grid synchronization and power factor issues. To overcome these drawbacks here introduced a novel fuzzy logic control topology. In this work tested the performance of proposed grid connected PV system under three conditions named normal operation, low voltage ride through (LVRT) and virtual synchronous generator (VSG). In the VSG topology PI controller is used to generate the reference currents. But by using of PI controllers will leads to low-speed response of the system. So, to overcome this issue, in the place of PI Controllers here introduced Fuzzy Logic Controllers. The proposed Fuzzy Logic Controllers will provide solutions to complex problems, robust, simple, and can be modified according to our requirements which will gives us accurate output. So, the speed response of the system will increase. The entire proposed system implemented and tested in MATLAB/SIMULINK.

Keywords: Impedance-source inverter, virtual synchronous generator, photovoltaic (PV) systems, low voltage ride through, fuzzy logic controller.

I. INTRODUCTION

Electrical energy is increasingly in demand. The issue of finite reservoirs, which could run dry in the next decades, is a severe one for traditional energy sources like thermal and others. The environment is seriously threatened by the carbon emissions from traditional power plants. Nuclear energy is another energy source that poses a major risk to people's safety. In the

recent years, experts have focused intensely on renewable energy sources in an effort to address the aforementioned issues. Solar energy is the most palatable option among all renewable energy sources because it is widely accessible and cost-free. Utilizing solar photovoltaic (PV) technology, solar energy is transformed into electrical energy. Solar PV, power electronics converters, and a control unit to manage the electricity obtained from solar PV make up the

entire solar energy conversion system. Nonlinear properties can be seen in solar PV cells. Its efficiency is quite low, and the DC power production changes depending on the ambient temperature and sun radiation [1]. Fixing the operating point at the maximum power of the PV curve is required to acquire the most electricity possible from solar PV under various environmental circumstances. Different methods are suggested, referred to as maximum power point tracking (MPPT) schemes, to accomplish this objective [1].

If it is effectively captured by contemporary technology, solar energy is the most effective form of renewable energy [1]. Sunlight is immediately turned into electrical energy in a solar PV system. A solar cell's capacity to produce energy largely depends on the cells' inherent characteristics and the amount of solar radiation that strikes the panel. The type of connected loads determines the average size of the solar array and the AC inverter needed for solar PV applications. Battery storage is another option for eventual usage of the panel's electricity. The main drawback of solar PV systems is their poorer efficiency because their panels are so heavily dependent on erratic meteorological variables like temperature and solar radiation. As a result, getting the most power possible from the panel is a little challenging, which lowers system efficiency. Different MPPT (Maximum Power Point Tracking) approaches are utilised to boost system efficiency and capture the most power possible from the panels [2].

The management of active and reactive power is fundamental and crucial for a PV system that is connected to the grid. The typical grid-connected PV system turns all of the radiation that is absorbed into active power, preventing the creation of reactive power. The benefit of this control technique is that users and designers can quickly assess system performance. The PV system does, however, progress toward greater capacity. The majority of large-scale PV facilities in China are typically installed in western regions. Some of them can only link to

nearby grid branches or are located far from the main grid. For these grid-connected PV systems, reactive power compensation and harmonic restriction have so emerged as crucial new technologies. The three-phase inverter's circuit topology matches that of the three-phase reactive power compensator. Through effective inverter current regulation, it can generate reactive power and lessen grid current distortion. Some studies have combined ZSI with the ability to compensate for reactive power or restrict harmonics. The shoot-through time was paired with sinusoidal pulse width modulation when driving power devices were modulated (SPWM). To measure the current harmonics, three-phase load currents on the d-q coordinates are used [3].

Virtual synchronous generators (VSGs) are designed to address these issues. With an increasing number of VSGs connected to the microgrid, stability issues have received considerable attention, with particular emphasis on a single VSG and paralleled VSGs. However, because VSGs are inverters with low over-current capabilities, they are susceptible to physical damage and must be protected through control switching or even forced outages in the event of a severe disturbance. As a result, dependable power sources are required to keep an islanded micro grid's frequency and voltage stable. Synchronous generator (SG)-based DERs are a common and widely used reliable power source in a Consortium for Electric Reliability Technology Solutions (CERTS) microgrid. As a result, a paralleled synchronous and virtual synchronous generators (SG-VSG) system exists in microgrids, and its stability issues must be investigated, particularly under large disturbances. More importantly, the transient instability mechanism of paralleled SG-VSG systems is more complicated than that of a single VSG or paralleled VSGs, making system planning and design more difficult, and even endangering system security [4].

The VSG is made up of three parts: energy storage, an inverter, and a control mechanism. Typically, the VSG is located between a DC bus/source/DG and the

grid. The VSG represents the DC source to the grid as an SG in terms of inertia and damping. Actually, the system emulates virtual inertia by controlling the active power through the inverter in inverse proportion to the rotor speed. Aside from higher frequency noise caused by inverter power transistor switching there is no difference in the electrical appearance of an electromechanical SG and an electrical VSG from a grid perspective [5].

However, the stable operation and control performance under grid fault must be taken into consideration when employing VSG technology for distributed power supply and microgrid for grid-connected operation. It was suggested to use smooth switching-based low-voltage ride through (LVRT) control for VSG, and a thorough explanation of the smooth handoff algorithm between modes was provided. The transient switching mechanism was not thoroughly analysed in this scheme, and it was not shown that the system could emulate the operational benefits of SG in the event of a grid breakdown. To provide an auxiliary explanation for the stability of the control method, the negative inertia of VSG was provided. This has significant educational value for future research. A virtual current source must be used to transform the converter into a controlled current source. The unique LVRT control approach for VSG proposed in this paper is based on the system excitation state. This study especially examines the response traits of VSG during LVRT in an effort to pinpoint the underlying reason of LVRT insufficiency. The concept of state maintenance is applied in VSG under LVRT in order to fully inherit the findings of previous research, and the control structure of VSG is enhanced to eliminate the additional smooth handoff algorithm [6].

However, this control strategy was presented only from the perspective of current limiting, and did not involve the response characteristic analysis of VSG under grid fault. Besides, only a few of above literatures have used the existing operational experiences of SG to analyse and improve the

performance of VSG. The authors in [7, 8] put forward excellent LVRT schemes for doubly fed induction generator, but it still needs to provide strict theoretical analysis of the VSG. In [9, 10], virtual current loop was used to make the converter act as a controlled current source. However, VSG is a voltage source grid-connection algorithm. The current loop should be improved to transmit the voltage source output characteristics.

To overcome all the above mentioned drawbacks a novel topology of dual mode operation and control of fuzzy logic controller based Z-source virtual synchronous generator in solar PV system is introduced in this paper. The remaining sections incorporated as follows. Section. II System description about principle of operation and control modes, section III. Proposed topology, section.IV results and discussion, section V. conclusion.

II. SYSTEM DESCRIPTION

A) PRINCIPAL OPERATION OF ZSI

ZSI employs shoot-through states, in which the load terminals are short-circuited via the lower and upper switches of any phase leg. This state does not apply to conventional voltage source inverters because the dc link is shorted and the converter is damaged [11]. As a result, switches in a ZSI do not require any dead time because they can use all possible switching combination states. As a result, the current distortion is reduced, and the total harmonic distortion of the current is expected to be lower. Furthermore, a boost capability for the ZSI is provided by varying the modulation index m of the inverter and the duration time of the shoot-through period. The ZSI, u_{abc} 's output voltage is calculated using (1):

$$B = \frac{V_{pn}}{V_{pv}} \quad (1a)$$

$$u_{abc} = m * B \frac{V_{pv}}{2} \quad (1b)$$

Where B indicates the boosting factor, V_{pv} indicates the input dc voltage, and V_{pn} indicates the impedance network output voltage. If, in a

symmetrical topology, $L_1 = L_2$, and $C_1 = C_2$, then (2) maintains as follows:

$$VC_1 = VC_2 = VC_3$$

$$iL_1 = iL_2 = iL \quad (2)$$

Where the impedance network's capacitor voltage and inductor current, respectively, are denoted by V_C and i_L . The input-output relations for a ZSI are demonstrated in by formulating volt-second and capacitor-charge average equations for inductor voltage and capacitor current (3)

$$V_{pn} = \frac{V_{pv}}{1-2D_0} = \frac{V_c}{1-D_0} \quad (3a)$$

$$V_c = \frac{1 - D_0}{1 - 2D_0} V_{pv} \quad (3b)$$

It has a non-shoot-through duty ratio of $D_0 = 1$ and a shoot-through duty ratio of $D_0 = 0$. In order to maintain a sufficient voltage control margin, D_0 must be smaller than or equal to (1 m) in this paper's simple boost modulation approach.

B) PROPOSED CONTROL MODES OF OPERATION

The suggested ZVSG converter can function in a variety of situations. The PV system is running under the MPPT state when it is in its typical operating mode (rated frequency and voltage). Therefore, the control system must decrease the active power generated and boost the reactive power. Using the grid codes and the system requirements as a guide, calculate the new references for active and reactive power.

A. PROPOSED CONTROL UNDER NORMAL OPERATION

1) DC SIDE CONTROL

As shown in Fig. 1 the perturb and observe (P&O) algorithm implements the MPPT. A PI controller is used to determine the shoot-through duty D_0 in order to manage the output voltage of the impedance network, V_{pn} , after comparing the measured voltage of the PV array, V_{PV} , with the reference voltage at the maximum power point, V_{MPP} .

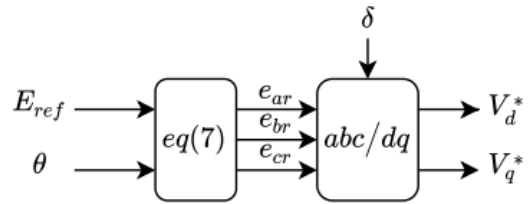


FIGURE 1. The generated outer loop reference voltage by using the VSG reference angle θ , and the reference voltage amplitude E_{ref}

2) AC SIDE CONTROL

In order to produce a reference angle, the swing equation of the SG is first numerically solved in each calculation cycle. Second, a three phase reference voltage is created using the estimated angle. A SG's mechanical equation is given by (4):

$$\frac{d\theta}{dt} = \omega \quad (4a)$$

$$2H \frac{d\omega}{dt} = T_m - T_e - D_p \Delta \omega \quad (4b)$$

Where D_p is the power damping coefficient, ω is the angular frequency, and H is the inertia time constant. T_e and T_m are the mechanical and electromagnetic output torques depicted in (5):

$$T_m = K_f(f_0 - f) + \frac{P_{ref}}{\omega} \quad (5a)$$

$$T_e = \frac{P_e}{\omega} \quad (5b)$$

where P_e and P_{ref} represent the measured and reference active power of the PV output, k_f the active power droop coefficient, and f_0 and f the system's rated and measured frequencies, respectively. The VSG algorithm's reference voltage magnitude, E_{ref} , is determined as follows in (6):

$$E_{ref} = E_0 + E_Q \quad (6)$$

E_Q is set to 0 since no reactive power is added to the grid. The three phase reference voltage of the ZVSG can be determined in (7) using E_{ref} as the reference voltage amplitude and the calculated reference angle in (4):

$$E_{ref} = \begin{bmatrix} e_{ar} \\ e_{br} \\ e_{cr} \end{bmatrix} = \begin{bmatrix} E \sin(\omega t) \\ E \sin(\omega t - \frac{2\pi}{3}) \\ E \sin(\omega t + \frac{2\pi}{3}) \end{bmatrix} \quad (7)$$

EQ is set to 0 since no reactive power is added to the grid. The three phase reference voltage of the ZVSG can be determined in (7) using Eref as the reference voltage amplitude and the calculated reference angle in (4):

$$T_{abc/dq} = \sqrt{\frac{2}{3}} \begin{bmatrix} \cos(\delta) \cos(\delta - \frac{2\pi}{3}) \cos(\delta + \frac{2\pi}{3}) \\ -\sin(\delta) - \sin(\delta - \frac{2\pi}{3}) - \sin(\delta + \frac{2\pi}{3}) \end{bmatrix} \quad (8)$$

In order to determine the input angle (δ) for this transformation, a Virtual Flux Orientation Control (VFOC) approach is used, and the calculated voltage in (7) serves as the reference for the outer voltage loop.

C) VIRTUAL FLUX ORIENTATION CONTROL

The VSG control method depends on the frequency and the proper phase angle of the grid at each time instant to determine the operating point of the converter during synchronisation in the event of load fluctuations. This angle is often measured via a phase locked loop (PLL), in which the frequency and phase angle are derived from the measured voltage of the grid. This angle is provided into the Park transformation as an input angle (V_{abc}). Under normal voltage settings, this voltage-oriented control technique utilised in PLL performs admirably, but when the grid voltage contains additional harmonics, its performance degrades.

Virtual flux is determined by computing the grid voltage integral (V_{abc}) as shown in equation (9) :

$$\psi_{abc} = \int V_{abc} \cdot dt. \quad (9)$$

The input angle is determined in (10) to get the position angle for the Park transformation after the reference frame of "abc" has been altered using the Clarke transformation.

$$\delta = \tan^{-1} \frac{\psi_{\beta}}{\psi_{\alpha}} \quad (10)$$

In this paper, a robust virtual flux calculation is hired as shown in (11):

$$g_3(s) = \frac{\psi(s)}{V(s)} = G_{BPF}(s) \cdot G_c(s) = \frac{K_B^S}{s^2 + (\frac{\omega_b}{Q_b})s + W^2} \cdot \frac{1 + \tau s}{1 + \lambda \tau s} \quad (11)$$

B) GRID CONNECTION PRE-SYNCHRONIZATION

As a result, a pre-synchronization technique is required that transforms each state variable into a single SRF. In this study, a VFOC-based control is used to monitor the grid voltage's phase, as shown in Fig. 5. Adjusting the relative phase difference (1) between the grid and the ZVSG's output voltage is the aim of this control. As depicted in Fig.2

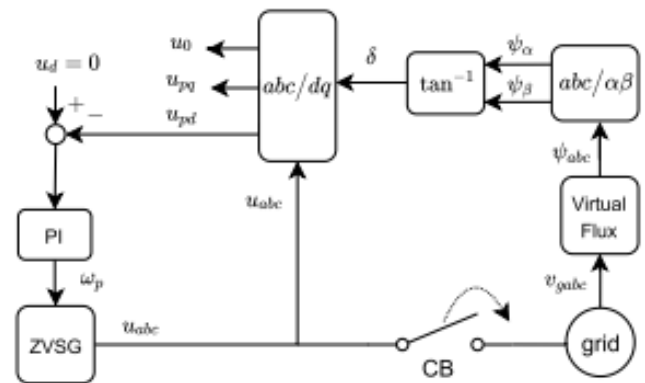


FIGURE 2. The VFOC based pre-synchronising control process

This objective is achieved by sending u_d to a PI controller, which compares it to a fixed zero reference and produces the angular frequency compensation ω_p in (12)

$$\omega_p = - \left(K_{pp} U_{pp} + \int K_{p1} U_{pd} dt \right) \quad (12)$$

III. PROPOSED TOPOLOGY

The Fuzzy Logic Controllers will provide solutions to complex problems, robust, simple, and can be modified according to our requirements which will gives us accurate output.so, the speed response of the system will increase. The simulation results of this system are evaluated by using Matlab/Simulink Software. The implementation of FLC is easy to design and it is not that much of easy to use because it requires a qualitative knowledge. It mainly consists of two inputs namely error and change in error and one

output which are depicted in below figures. In this work, FLC is employed.

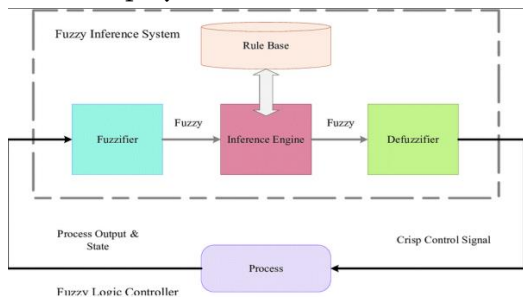


Fig 3. Fuzzy logic controller:

e/ce	NB	N	Z	P	PB
NB	PB	PB	P	Z	Z
N	P	P	Z	Z	Z
Z	Z	Z	Z	Z	Z
P	Z	Z	N	N	N
PB	N	N	N	NB	NB

Table 1. Rules table

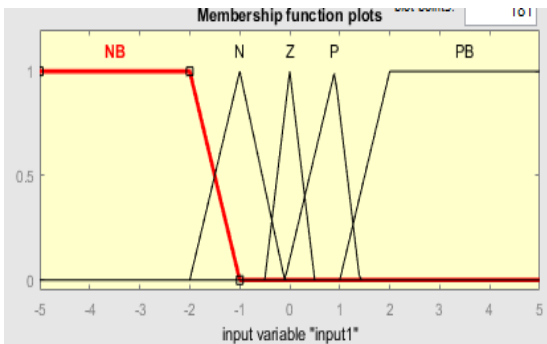


Fig 4. VOLTAGE error

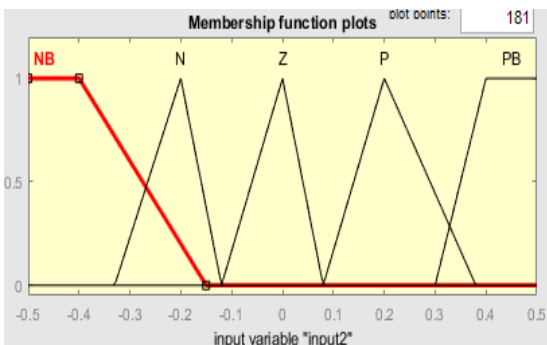


Fig 5. VOLTAGE change in error

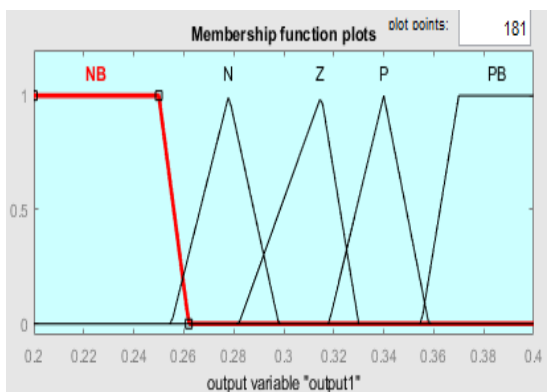


Fig 6. Reference CURRENT

IV. RESULTS AND DISCUSSION

4.1 simulation results using PI controller

A) Frequency regulation

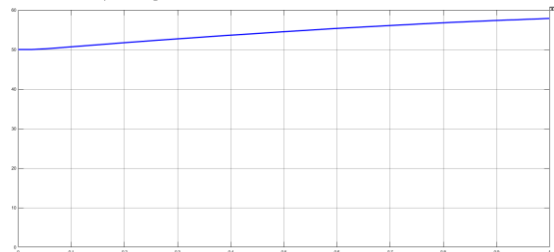


Fig 7a.

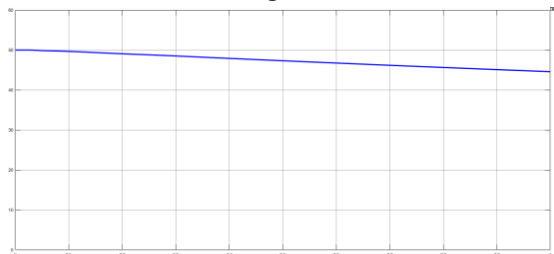


Fig 7b.

FIGURE 7 RoCoF curves with different amounts of (a) inertia (H) and (b) damping constant (DP).

At this time, the ZVSG is operating in MPPT mode, and Fig. 9 shows RoCoF charts for the converter. Active load rose by 0.2 p.u. at time $t = 1$ sec. The RoCoF is depicted in Fig. 7a with various values of (H), where the larger the RoCoF curve is for lower values of H. The system is more vulnerable due to the larger RoCoF, which might also be because RoCoF relays to activate and disconnect the DGs from the grid. For adjusting the damping constant, D_p of the system as

indicated in Fig. 7b, the identical outcomes are perceptible.

B. GRID CONNECTION

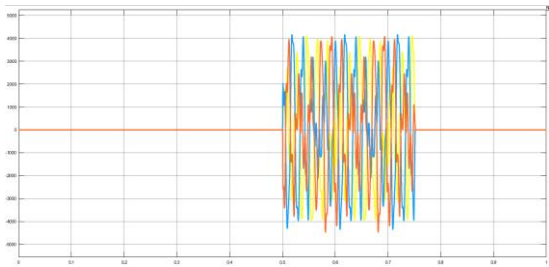


Fig 10a.

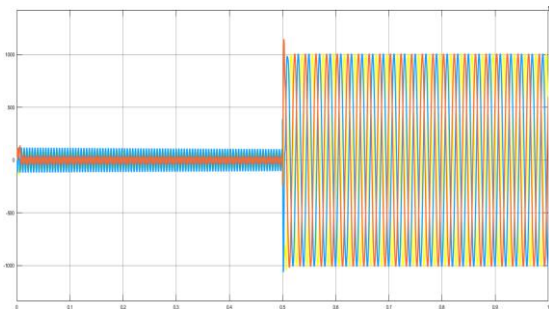


Fig 10b.

FIGURE 10. Comparison in ZVSG current increase while (a) the converter is directly connected ($100(\text{mA}) * 3.2 * 10000 = 3200\text{A}$) and (b) a pre-synchronizing control method is hired to decrease the current increment ($200(\text{mA}) * 1 * 5000 = 1000\text{A}$).

The ZVSG's overcurrent current upon connecting to the grid is depicted in Fig. 10. When ZVSG is connected to the grid without any pre-synchronization control, Fig. 10a depicts the current waveform; nevertheless, Fig. 10b depicts the same waveform after employing the suggested pre-synchronization approach.

C. VOLTAGE REGULATION

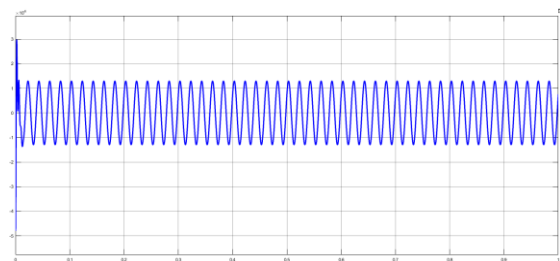


Fig 11.a

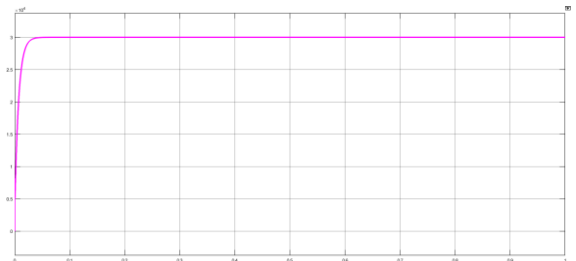
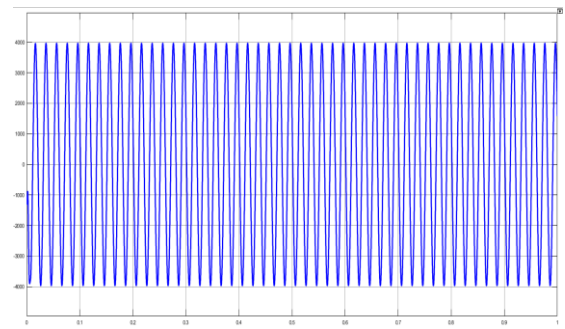


Fig 11b

FIGURE 11(a) (b) Multi-mode operation of the ZVSG during (a) normal operation

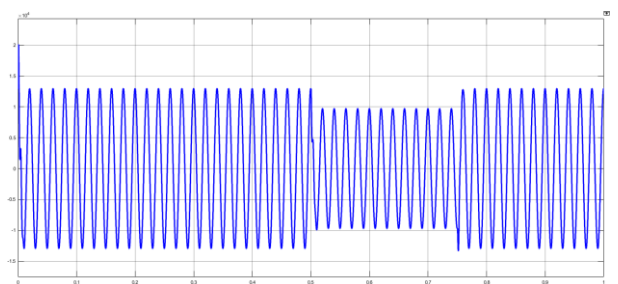


Fig 11c.

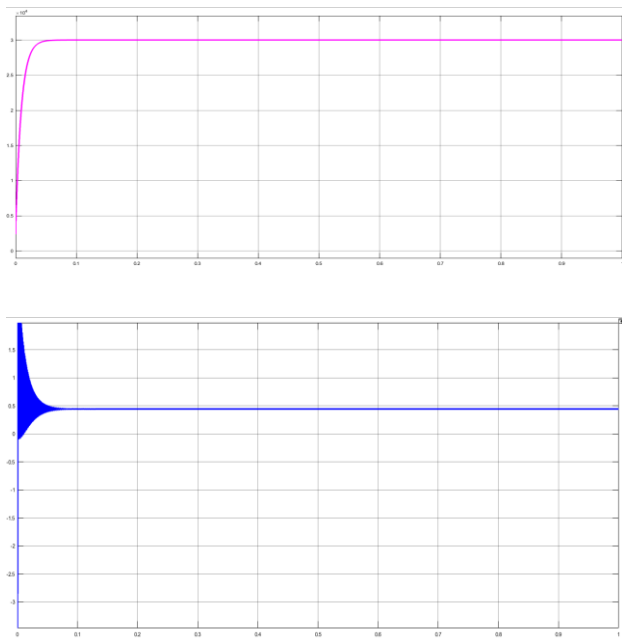


Fig 11d.

Figure 11 depicts the overall system performance prior to the fault and following its repair. First, in this case study, the system is operating normally and with a power factor of one. Grid setup similar to that in Fig. 11a. The grid voltage is at t_1 due to a three phase malfunction, decreased to 0.75 percent of its rated value. According to Fig. 11c. The voltage is detected by the sag detector. Reduction and changes the operation mode of the LVRT controller new references for the active and reactive modes. Depending on the grid codes and the seriousness of the drop in voltage. Therefore, the ZVSG injects reactive power to the grid that results in recovering the voltage at t_2 as shown in Fig. 11d.

4.2. Simulation results by using fuzzy logic controller

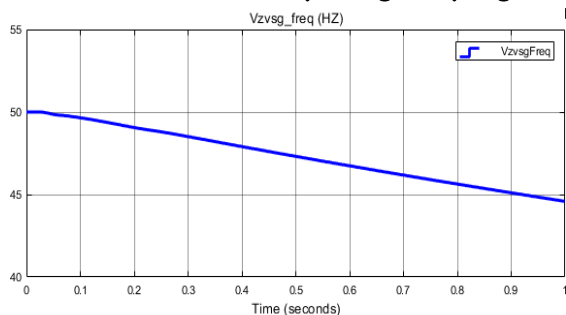


Fig 12.Frequency at ZVSG side

The ZVSG is working under MPPT operation mode and RoCoF plots of the converter are depicted in Fig. 12 by using ANFIS controller

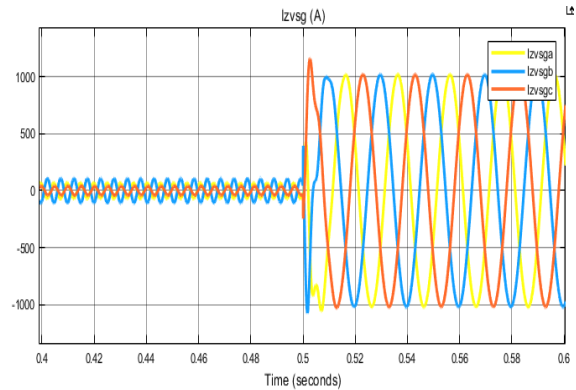


Fig 13.Izvsq

Fig. 13 shows the inrush current of the ZVSG while connecting to the grid by using Fuzzy logic controller.

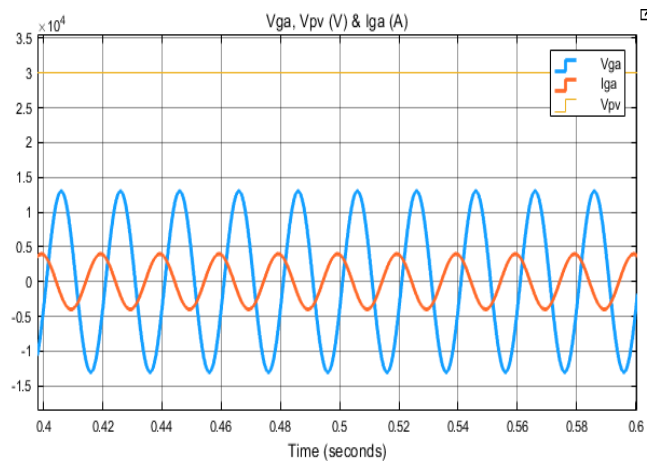


Fig 14.Vga, Vpv Iga

By using ANFIS controller the Fig. 13 shows the overall system performance before the fault and after recovering from it.

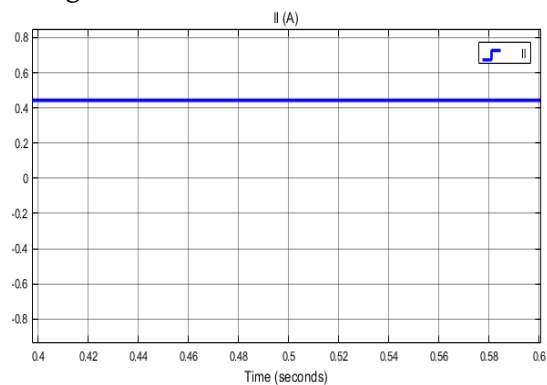


Fig 15. IL (A)

The above figure depicts current value of load by using fuzzy logic controller

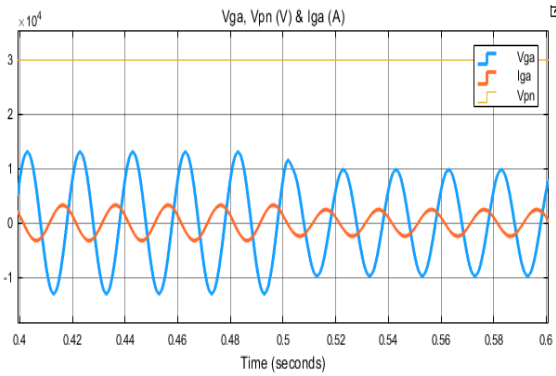


Fig. 16 Vga, Vpn & Iga

The above figure depicts performance of dc link voltage, inductor current and grid voltage by using fuzzy logic controller.

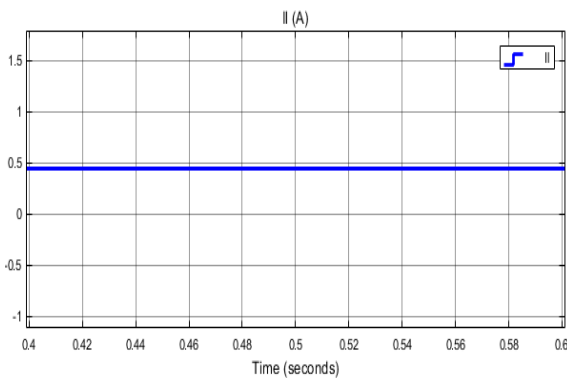


Fig 17. IiL (A)

The above figure depicts current value of load by using fuzzy logic controller

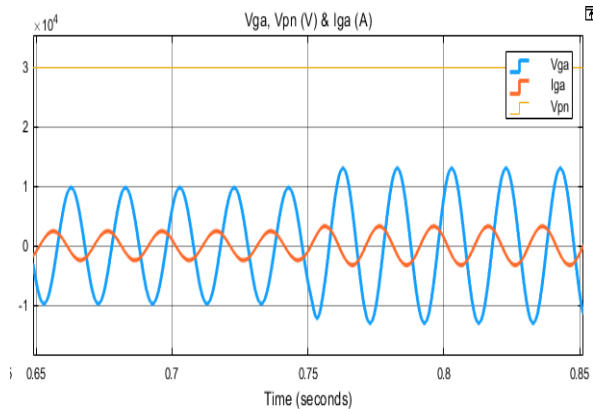


Fig 18. Vga, Vpn, & Iga (A)

The above figure depicts performance of dc link voltage, inductor current and grid voltage by using fuzzy logic controller.

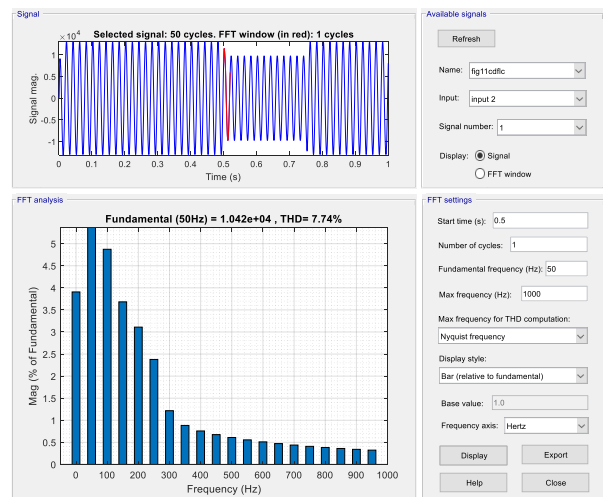


Fig 19(a)

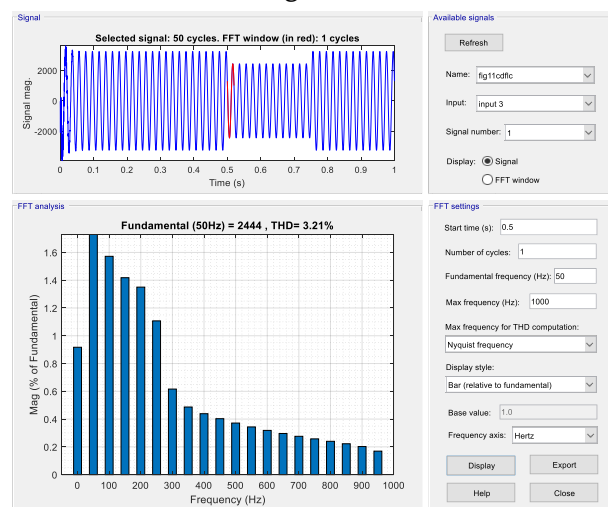


Fig 19(b)

The above figure 19a) & 19b) depicts the THD comparison by using fuzzy logic controller.

V. CONCLUSION

In this research work implemented a Dual mode operation and control of Fuzzy Logic Controller based Z-source Virtual Synchronous Generator in Solar PV system. By using the proposed fuzzy logic controller the voltage stability is maintained well under Sag or Swell conditions and also improved power factor while compared to conventional PI controller. The simulation results and discussion gives a solution for voltage stability, power factor issues and grid synchronization improvement in this research work.

VI. REFERENCES

- [1] Ahteshamul Haque1 and Zaheeruddin, "Research on solar photovoltaic (pv) energy conversion system" IEEE Transaction on Industrial Electronics, vol. 58, no. 4.
- [2] Kartika Dubey, M.T.Shah, "design and simulation of solar pv system" 978-1-5090-2080-5/16/\$31.00 ©2016 IEEE.
- [3] Jingwei Zhang, "Unified control of Z-source grid-connected photovoltaic system with reactive power compensation and harmonics restraint" IET Renew. Power Gener. 2018, Vol. 12 Iss. 4, pp. 422-429 © the Institution of Engineering and Technology 2017.
- [4] Huijie Cheng, Zhikang Shuai, Zuyi Li, "Transient Angle Stability of Paralleled Synchronous and Virtual Synchronous Generators in Islanded Microgrids" 2019 IEEE. Personal use is permitted, but republication/redistribution requires IEEE permission.
- [5] Jia Liu, Hassan Bevrani, Toshifumi Ise, "Enhanced Virtual Synchronous Generator Control for Parallel Inverters in Microgrids" 1949-3053 c 2016 IEEE.
- [6] Kai Shi , Haihan Ye , Peifeng Xu , Dean Zhao , Long Jiao," Low-voltage ride through control strategy of virtual synchronous generator based on the analysis of excitation state" IET Gener. Transm. Distrib. 2018, Vol. 12 Iss. 9, pp. 2165-2172.
- [7] H. M. Hasanien, "An adaptive control strategy for low voltage ride through capability enhancement of grid-connected photovoltaic power plants," IEEE Trans. Power Syst., vol. 31, no. 4, pp. 3230–3237, Jul. 2016.
- [8] M. Choopani, S. H. Hosseinian, and B. Vahidi, "New transient stability and LVRT improvement of multi-VSG grids using the frequency of the center of inertia," IEEE Trans. Power Syst., vol. 35, no. 1, pp. 527–538, Jan. 2020.
- [9] K. Shi, H. Ye, P. Xu, D. Zhao, and L. Jiao, "Low-voltage ride through control strategy of virtual synchronous generator based on the analysis of excitation state," IET Gener., Transmiss. Distrib. vol. 12, no. 9, pp. 2165–2172, 2018.
- [10] W. Li, J. Lv, X. Jiang, X. Zhang, and S. Sheng, "LVRT control method of flywheel energy storage system based on VSG," in Proc. IEEE 8th Int. Conf. Adv. Power Syst. Autom. Protection (APAP), Oct. 2019, pp. 1436–1440.
- [11] J. Liu, J. Hu, and L. Xu, "Dynamic modeling and analysis of Z-source converter—Derivation of AC small signal model and design-oriented analysis," IEEE Trans. Power Electron., vol. 22, no. 5, pp. 1786–1796, Sep. 2007.

Cite this article as :

D. Jaswanth, K. Siva Kumar, "Dual mode operation and control of Fuzzy Logic Controller based Z-source Virtual Synchronous Generator in Solar PV System", International Journal of Scientific Research in Science and Technology (IJSRST), Online ISSN : 2395-602X, Print ISSN : 2395-6011, Volume 10 Issue 1, pp. 476-485, January-February 2023.

Journal URL : <https://ijsrst.com/IJSRST2310143>